THE JOURNAL OF BIOLOGICAL CHEMISTRY VOL. 286, NO. 16, pp. 14271–14281, April 22, 2011

Phosphate-responsive Signaling Pathway Is a Novel Component of NAD$^+$ Metabolism in *Saccharomyces cerevisiae*[*][S]

Received for publication, December 31, 2010, and in revised form, February 23, 2011 Published, JBC Papers in Press, February 24, 2011, DOI 10.1074/jbc.M110.217885

Shu-Ping Lu and Su-Ju Lin[1]

From the Department of Microbiology, College of Biological Sciences, University of California, Davis, California 95616

Nicotinamide adenine dinucleotide (NAD$^+$) is an essential cofactor involved in various cellular biochemical reactions. To date the signaling pathways that regulate NAD$^+$ metabolism remain unclear due to the dynamic nature and complexity of the NAD$^+$ metabolic pathways and the difficulty of determining the levels of the interconvertible pyridine nucleotides. Nicotinamide riboside (NmR) is a key pyridine metabolite that is excreted and re-assimilated by yeast and plays important roles in the maintenance of NAD$^+$ pool. In this study we establish a NmR-specific reporter system and use it to identify yeast mutants with altered NmR/NAD$^+$ metabolism. We show that the phosphate-responsive signaling (*PHO*) pathway contributes to control NAD$^+$ metabolism. Yeast strains with activated *PHO* pathway show increases in both the release rate and internal concentration of NmR. We further identify Pho8, a *PHO*-regulated vacuolar phosphatase, as a potential NmR production factor. We also demonstrate that Fun26, a homolog of human ENT (equilibrative nucleoside transporter), localizes to the vacuolar membrane and establishes the size of the vacuolar and cytosolic NmR pools. In addition, the *PHO* pathway responds to depletion of cellular nicotinic acid mononucleotide (NaMN) and mediates nicotinamide mononucleotide (NMN) catabolism, thereby contributing to both NmR salvage and phosphate acquisition. Therefore, NaMN is a putative molecular link connecting the *PHO* signaling and NAD$^+$ metabolic pathways. Our findings may contribute to the understanding of the molecular basis and regulation of NAD$^+$ metabolism in higher eukaryotes.

NAD$^+$ and its reduced form NADH are essential pyridine nucleotides mediating redox reactions in cellular metabolism. In addition, NAD$^+$ is an essential substrate in several protein modification reactions, in particular sirtuin-mediated protein deacetylation and the addition of ADP-ribose moieties. These modifications are essential for the proteins functioning in Ca^{2+} signaling, chromatin structure, DNA repair, and lifespan (1–5). The cellular pool of NAD$^+$ is maintained by biosynthesis from nicotinic acid mononucleotide (NaMN)[2] or nicotinamide mononucleotide (NMN) (Fig. 1*A*). The production of NaMN involves the transfer of phosphoribose moiety from phosphoribose pyrophosphate to nicotinic acid (NA) catalyzed by Npt1 or to quinolinic acid (QA) by Qpt1 (6–8) (Fig. 1*A*). QA and NA are intermediate metabolites generated by *de novo* synthesis or by salvaging reactions that utilize exogenous pyridines or internal pyridines derived from NAD$^+$ utilizing reactions. In yeast, synthesis of NMN is achieved by Nrk1-mediated phosphorylation of nicotinamide riboside (NmR) at the expense of ATP (9, 10). NmR is a recently identified endogenous precursor for NAD$^+$ synthesis and the salvage of endogenous NmR is important in maintaining NAD$^+$ homeostasis and lifespan (11, 12). Because yeast cells constantly release and re-assimilate NmR, it has been suggested that this NmR pool might confer metabolic flexibility for prompt adjustment of cellular NAD$^+$ levels (11, 12). Although the NA/nicotinamide (Nam) salvage pathway appears to be the dominant route of NAD$^+$ synthesis when exogenous pyridine is available (13), the NmR salvage pathway also contributes significantly to the NAD$^+$ pool and supports NAD$^+$-dependent reactions (9, 10). It remains unclear how NmR is produced and how its metabolism is regulated in response to different growth conditions.

Inorganic phosphate (P_i) is essential for biomolecule synthesis, energy metabolism, and protein modification. The sensing, acquisition, and storage of P_i are mainly mediated by the phosphate-responsive signaling (*PHO*) pathway that controls P_i transporters, regulatory factors, and effectors (Fig. 1*B*) (14–16). When P_i availability is high, the downstream components of the *PHO* pathway are repressed mainly by the cyclin-dependent kinase complex (Pho80-Pho85), which phosphorylates and inactivates the major transcription factor Pho4. Upon P_i limitation, the synthesis of inositol heptakisphosphate (IP_7) was found to be increased (17, 18). It has been shown that inositol heptakisphosphate allosterically binds to the tertiary complex of Pho81 (a cyclin-dependent kinase inhibitor)-Pho80-Pho85 and induces a conformational change of Pho81 that prevents the phosphorylation of Pho4 by Pho85 (19). Unphosphorylated Pho4 accumulates in the nucleus and cooperates with another transcription factor Pho2 to activate *PHO*-responsive genes whose expression products include high affinity P_i transporters (Pho84 and Pho89), repressible phosphatases (Pho5 and Pho8), and factors for phosphate mobilization from vacuolar polyphosphate storage. It is not yet fully understood how cells

* This work was supported, in whole or in part, by National Institutes of Health Grant AG24351 (NIA).

[S] The on-line version of this article (available at http://www.jbc.org) contains supplemental Table 1.

[1] To whom correspondence should be addressed: Dept. of Microbiology, University of California, One Shields Ave., Davis, CA 95616. Tel.: 530-754-6082; Fax: 530-752-9014; E-mail: slin@ucdavis.edu.

[2] The abbreviations used are: NaMN, nicotinic acid mononucleotide; NA, nicotinic acid; QA, quinolinic acid; *PHO*, phosphate-responsive signaling; YPD, yeast extract-peptone-dextrose; Low-P_i, low phosphate; ENT, equilibrative nucleoside transporter; Nam, nicotinamide; NmR, nicotinamide riboside.

sense the level of phosphate availability to elicit proper metabolic responses. Interestingly, the *pho84*Δ mutant shows constitutive expression of *PHO5* (20, 21). It was shown that the defect in phosphate transport caused by *PHO84* mutations resulted in a low level of intracellular phosphate that led to constitutive de-repression of the *PHO* pathway and its downstream genes (22, 23). In addition to the changes of P_i availability, recent studies have shown that the *PHO* signaling pathway also responds to the alterations of intermediate metabolites in purine synthesis pathway in an inositol heptakisphosphate-independent manner (24, 25).

Due to the dynamic nature and redundancy of NAD$^+$ synthesis pathways, to date the signaling pathways that regulate NAD$^+$ metabolism remain unclear. One major barrier has been the lack of a specific and sensitive genetic screen system. Because yeast cells constantly release and retrieve NmR (11, 12), we reasoned that the changes in NmR release activity might reflect the alterations of cellular NAD$^+$ metabolism. In this study we employed a unique NmR reporter-based genetic screen to identify novel components and regulators of NAD$^+$ biosynthesis to elucidate the regulation of this pathway. We showed that components of the *PHO* pathway played important roles in NAD$^+$ metabolism. We also further characterized the molecular basis underlying the interconnection between these two pathways.

EXPERIMENTAL PROCEDURES

Yeast Strains, Growth Media, and Plasmids—Yeast strain BY4742 *MATα his3Δ1 leu2Δ0 lys2Δ0 ura3Δ0* acquired from Open Biosystems was used for this study (26). Yeast extract-peptone-dextrose (YPD) medium was made as described (27). Low phosphate (Low-P_i) medium was prepared by phosphate precipitation from YPD as previously described (28). In brief, for each liter of Low-P_i YPD medium, 10 g of yeast extract, 20 g of peptone, and 2.46 g of $MgSO_4$ were first dissolved in deionized water. 8 ml of concentrated ammonia was then slowly added with gentle stirring to precipitate inorganic phosphate as $MgNH_4PO_4$. After filtration, the clear solution was adjusted to pH 7 with HCl and subjected to autoclave. To prepare media with various concentrations of phosphate, Low-P_i YPD was supplemented with KH_2PO_4 to indicated concentrations. All gene deletions were generated by replacing wild type genes with a reusable loxP-*Kan^r*-loxP cassette as described (27). The Qpt1 overexpression construct p*ADH1*-Qpt1 was made in the integrative pPP81 (*LEU2*) vector as described (27). The resulting construct was verified by DNA sequencing.

Genetic Screen Using the Yeast Deletion Collection—The haploid yeast deletion collection (~4500 strains) established in the BY4742 background was acquired from Open Biosystems (29). To screen for mutants with altered NmR release, 2 μl of each strain was directly taken from the frozen stock and then spotted onto YPD plates spread with NAD$^+$ auxotrophic recipient cells (the *npt1*Δ*qpt1*Δ mutant) at a density of ~9000 cells/cm^2. The growth of the recipient cells relies on the NmR released from the interested NAD$^+$ prototrophic strains, which also indicates the levels of NmR release. After incubation at 30 °C for 3 days, we scored the cross-feeding activity of each strain from the mutant collection by comparing the diameter of the cross-feeding zones to that of the wild type. Mutants with increased cross-feeding activities showed larger cross-feeding zones and were assigned positive numbers with higher magnitude indicating stronger phenotype (+1 ~ +5). Mutants with decreased cross-feeding activities were assigned negative scores (−1 ~ −5). We further confirmed the hits with scores higher than +2 or lower than −2. Cells from the frozen stock were first recovered in fresh medium for 2 days. 2×10^4 cells of each strain were then spotted and scored as described above. The final scores were calculated by summing scores assigned in two screens. The Saccharomyces Genome Data base was then consulted to organize the candidates by molecular functions as shown in supplemental Table 1.

Determinations of Extracellular and Intracellular NmR—NmR levels were determined by liquid-based cross-feeding bioassay using NAD$^+$ auxotrophs as reporter cells whose growth reflects the level of NmR in the medium (11). To prepare cell extracts for intracellular NmR determination, 10 ml of cells (the donor of interest) grown to late log phase (~24 h of growth from A_{600} of 0.1) were lysed by bead-beating in 800 μl ice-cold 50 mM ammonium acetate solution. After filter sterilization, 8 μl or 16 μl clear extract was used to supplement 8 ml culture of recipient cells (the *npt1*Δ*qpt1*Δ*pho5*Δ mutant) with starting A_{600} of 0.05 in YPD. To determine NmR release, cell-free supernatant of donor cell culture was collected, and 500 μl was used to feed recipient cells. A control culture of recipient cells in YPD without any supplementation was included in all experiments. After incubation at 30 °C for 24 h, growth of the recipient cells (A_{600}) was measured and normalized to the cell number of donor strain.

NmR, NaR, NMN, NaMN, and NAD$^+$ Measurements by LC-Mass Spectrometry—Total intracellular levels of NAD$^+$ metabolites were prepared and determined by LC-mass spectrometry as described (11) at the metabolomics core laboratory at UC Davis. One major difference was that we previously analyzed cells grown to late log phase (a 16-h culture starting with a A_{600} of 0.1) (11). In this study we analyzed cells grown for 24 h, the time point when cellular NmR production reached the maximum level (data not shown). Cell extracts were prepared from 10^{10} cells by bead-beating in ice-cold 50 mM ammonium acetate solution (30). Samples were freeze-dried at −80 °C and then were resuspended in 500 μl of MeOH:H_2O (4:1, v/v). 5 μl was used for LC-MS analysis. Chemically synthesized NmR, NaR (both were kindly provided by Dr. A. Sauve), NaMN (Sigma), NMN (Sigma), and NAD$^+$ (Roche Applied Science) were used to establish standard curves. Detection and quantification were performed as described (31).

Repressible Acid Phosphatase Activity Assay—The color-forming repressible acid phosphatase plate assay was carried out as described previously (32) with modifications. 1.6×10^4 cells and a 5-fold dilution were spotted on YPD plates. After incubation at 30 °C for 3 days, colonies were overlaid with molten 1% soft agar containing 1.1 mg/ml α-naphthol phosphate (Sigma) and 0.73 mg/ml Fast blue B salt (Sigma) in 0.05 M sodium acetate buffer, pH 4. The intensity of color formation indicates the activity of secreted repressible acid phosphatase. The repressible acid phosphatase liquid assay was performed as described (32) on cells grown to late log phase in YPD. In brief,

~2.5 × 10^7 cells were harvested, washed, and resuspended in 150 μl of water. 600 μl of substrate solution (5.6 mg/ml *p*-nitrophenyl phosphate in 0.1 M sodium acetate, pH 4) was added to the cell suspension, and the mixture was incubated at 30 °C for 15 min. The reaction was stopped by adding 600 μl of ice-cold 10% trichloroacetic acid. 600 μl of this final mixture was then added to 600 μl of saturated Na_2CO_3 to allow color (neon yellow) development. Cells were pelleted to acquire the supernatant for A_{420} determination. The acid phosphatase activities were determined by normalizing A_{420} readings to cell number and are expressed as Miller units ($A_{420} \times 1000/(A_{600} \times \text{ml} \times 15$ min)) (33).

Fluorescence Microscopy—Strain expressing Fun26-GFP fusion protein was made by integrating *GAL1* promoter and GFP coding region to the immediate upstream of genomic *FUN26* gene using pFA6a-kanMX6-PGAL1-GFP as described (34). Proper integration was verified by PCR, and the function of Fun26 was confirmed by a cell-based cross-feeding assay (Fig. 4*C*). Localization analysis of Fun26-GFP was performed by fluorescence microscopy with a Nikon Eclipse 80i microscope at a ×1000 magnification.

Pho8-dependent Alkaline Phosphatase Activity Assay—The cell extract-based alkaline phosphatase activity assay was carried out as previously described (35) with modifications. 40 A_{600} units of cells grown in YPD for 24 h were collected and washed in 0.85% NaCl with phenylmethylsulfonyl fluoride as described (35). The resultant cell pellet was then resuspended in 500 μl of lysis buffer (20 mM PIPES, 0.5% Triton X-100, 50 mM KCl, 100 mM potassium acetate, 10 mM $MgSO_4$, 10 μM $ZnSO_4$, 1 mM phenylmethylsulfonyl fluoride) following by bead-beating. Cell lysates were then centrifuged at 14,000 × *g* for 5 min at 4 °C to collect supernatant. 100 μl of supernatant was added to 400 μl of reaction buffer (250 mM Tris-HCl, pH 8.5, 0.4% Triton X-100, 100 mM $MgSO_4$, 10 μM $ZnSO_4$, with/without 5 mM NMN) and then incubated at 37 °C for 20 min. Reactions were stopped by adding 500 μl of stop buffer (1 M glycine/KOH, pH 11.0). Supernatants were then collected by centrifugation. After filter sterilization, 100 μl of supernatant was used to supplement 8 ml of culture of recipient cells (the *npt1*Δ*qpt1*Δ*pho5*Δ mutant) with a starting A_{600} of 0.05 in YPD. After incubation at 30 °C for 24 h, growth of the recipient cells (A_{600}) was measured. Alkaline phosphatase activities toward NMN were expressed as NmR (nmol) produced in the reaction determined by a cross-feeding assay. A_{600} readings were converted to NmR levels using the cross-feeding-based NmR standard curve (Fig. 1*D*). Pho8 alkaline phosphatase activities toward NMN and NaMN were also determined by LC-mass spectrometry and expressed as the rate of NmR (for NMN) or NaR (for NaMN) produced in the reaction (nmol/μg of total protein/min).

RESULTS

The PHO Signaling Pathway Affects Both NmR Release and Intracellular NmR Levels—Wild type yeast cells constantly release NmR and re-assimilate it. The release of NmR was first detected by cell-based cross-feeding assays in which the growth of NAD$^+$ auxotrophic cells reflects the level of NmR released from neighboring NAD$^+$ prototrophic cells (11). To identify factors that regulate NmR/NAD$^+$ metabolism, we screened a collection of yeast deletion mutants (29) for defects in cross-feeding ability. After two rounds of screening, 140 mutants were identified and classified based on cross-feeding abilities and other nutritional phenotypes ("Experimental Procedures") (supplemental Table 1). Notably, the NmR assimilation mutant (*nrk1*Δ) (9) and NmR transport mutants (*nrt1*Δ and *fun26*Δ) (36) showed the strongest cross-feeding ability, validating the specificity of our screen (Group I, supplemental Table 1). In addition, three mutants with deletions of NAD$^+$ salvage enzymes (Npt1, Nma1, Hst1) (37–39), and eight mutants with deletions of purine synthesis enzymes also displayed significantly reduced cross-feeding activity (Group III and IV, supplemental Table 1). The identification of these NAD$^+$ synthesis enzymes suggested that our screen might have also uncovered additional novel components of NAD$^+$ metabolism.

Interestingly, defects in the phosphate signaling (*PHO*) pathway alter NmR release behavior (Group II and IV, supplemental Table 1). To verify that the observed phenotypes are due to the featured mutations and not to secondary cryptic mutations in the strain collection, we constructed new mutants with defects in the phosphate transporters or the *PHO* regulatory factors (Fig. 1*B*) for further analysis. Among the phosphate transport mutants, *pho84*Δ (major high affinity phosphate transporter) and *pho90*Δ (major low affinity phosphate transporter) showed modest increases in NmR release that were consistent with the screen results (Fig. 1*C*, *upper two panels*). Moreover, the *pho4*Δ and *pho2*Δ (*PHO*-regulated transcription factors) mutants displayed reduced NmR release, whereas the *pho85*Δ (inhibitor of Pho4) mutant showed increased NmR release (Fig. 1*C*, *lower two panels*). Because *pho84*Δ and *pho85*Δ both lead to de-repression of the *PHO* pathway (20, 21), our results showed a positive correlation between the level of NmR release and the *PHO* pathway activity.

To understand whether the *PHO* pathway activity also correlates with NmR production, we determined intracellular NmR levels of the *pho84*Δ (increased *PHO* activity) and *pho4*Δ (decreased *PHO* activity) mutants by a liquid-based cross-feeding bioassay ("Experimental Procedures"). In this assay the growth of the reporter cells (NAD$^+$ auxotroph) is dependent on NmR supplement in culture medium. We first established a dose-response standard curve to show the correlation between the growth of the reporter cells and the concentrations of supplemented NmR (Fig. 1*D*). Next, we determined intracellular NmR concentrations of the *PHO* mutants by supplementing reporter cells with the cell extracts prepared from these *PHO* mutants. As shown in Fig. 1*E*, intracellular NmR levels were significantly increased in the *pho84*Δ mutant and were attenuated by a *PHO4* deletion. Together, our studies demonstrate a positive correlation between NmR level and the activity of *PHO* pathway.

Phosphate Limitation Alters NmR Metabolism—We next tested whether cellular NmR level would respond to changes of P_i availability. As shown in Fig. 2*A*, wild type cells grown in Low-P_i medium showed a significant elevation in the level of intracellular NmR, whereas the level of released NmR appeared to be decreased. Cells grown in Low-P_i media re-supplemented with P_i also displayed an inverse correlation between P_i availability and intracellular NmR level (Fig. 2*B*). In addition, the

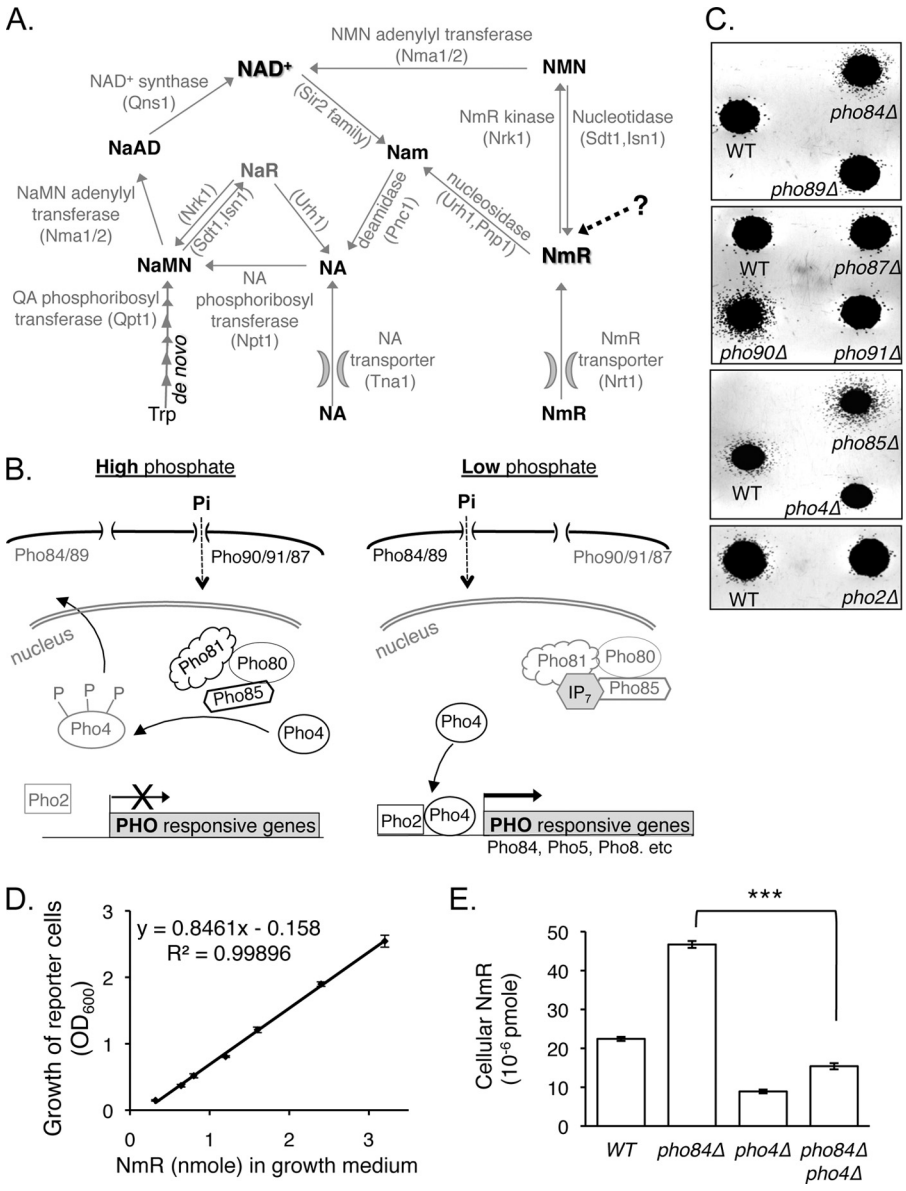

FIGURE 1. **NmR levels positively correlate with the *PHO* pathway activities.** *A*, the model of NAD$^+$ biosynthesis pathways in the yeast *Saccharomyces cerevisiae* consists of a *de novo* synthesis from tryptophan and the salvage of various NAD$^+$ precursors. In vertebrates including mammals, the involvement of Nam deamidase Pnc1 in Nam salvage is absent. Instead, the utilization of Nam is achieved by the addition of phosphoribose to make NMN, which is mediated by the Nam phosphoribosyl transferase (58). *NaR*, nicotinic acid riboside. *NaAD*, deamido NAD$^+$. Abbreviations of protein names are shown in parentheses. *B*, the *PHO* responsive signaling pathway is shown. The *PHO* signaling is normally repressed by a cyclin-cyclin-dependent kinase complex (Pho80-Pho85), which phosphorylates and inactivates the transcription factor Pho4. When phosphate is limiting, Pho81 (a cyclin-dependent kinase inhibitor) inhibits the Pho80-Pho85 complex, thereby derepressing *PHO*-responsive genes. The regulation of Pho80-Pho85 is distinct from typical cyclin-dependent kinase regulation; the cyclin-dependent kinase inhibitor Pho81 is constitutively associated with Pho80-Pho85, and inositol heptakisphosphate (IP_7) is required for Pho80-Pho85 inactivation. *Pho84/89*, high affinity P_i transporters; *Pho90/91/87*, low affinity P_i transporters; *Pho5 and Pho8*, repressible phosphatases. *C*, mutants with increased *PHO* activity release more NmR, whereas mutants with decreased *PHO* activity release less NmR compared with WT. The *upper two panels* show NmR release of mutants defective in high affinity phosphate transporters (*first panel*) or in low affinity phosphate transporters (*second panel*) determined by cross-feeding assay. The *lower two panels* show NmR release of mutants defective in the regulatory factors. Results show growth of the NAD$^+$ auxotrophic *npt1*Δ*qpt1*Δ recipient cells (plated on YPD at a density of ~9000 cells/cm^2) supported by feeder cells (the *PHO* mutants, ~2×10^4 cells spotted directly onto the recipient lawn). Cells were grown at 30 °C for 2 days. *D*, the correlation between the growth (A_{600}) of the NAD$^+$ auxotrophic *npt1*Δ*qpt1*Δ*pho5*Δ reporter cells and the level of supplemented NmR (nmol) in 8 ml of culture is shown. *E*, intracellular NmR levels also correlate with the *PHO* pathway activities. The levels of intracellular NmR are determined by supplementing reporter cells with cell extracts prepared from the strains of interest (cross-feeding bioassay, "Experimental Procedures"). Results of one representative set of three independent experiments are shown. The *error bars* denote S.D. The *p* values are calculated using Student's *t* test (***, $p < 0.005$).

intracellular NmR level of the *pho84*Δ (constitutively *PHO* active) mutant was not further increased by P_i limitation, suggesting the alterations in NmR levels induced by low P_i were signaled through the *PHO* pathway (Fig. 2*C*). Interestingly, a mutant that is completely defective for assimilation of NmR (*nrk1*Δ*urh1*Δ*pnp1*Δ) exhibited an increase in NmR level similar to that seen for the wild type during P_i limitation (Fig. 2*D*). Therefore, the elevation of intracellular NmR level induced by low P_i appears to be caused by increased NmR production rather than by attenuated NmR utilization. Collectively, these data suggest that cellular NmR level could be modulated by P_i availability via the *PHO* pathway.

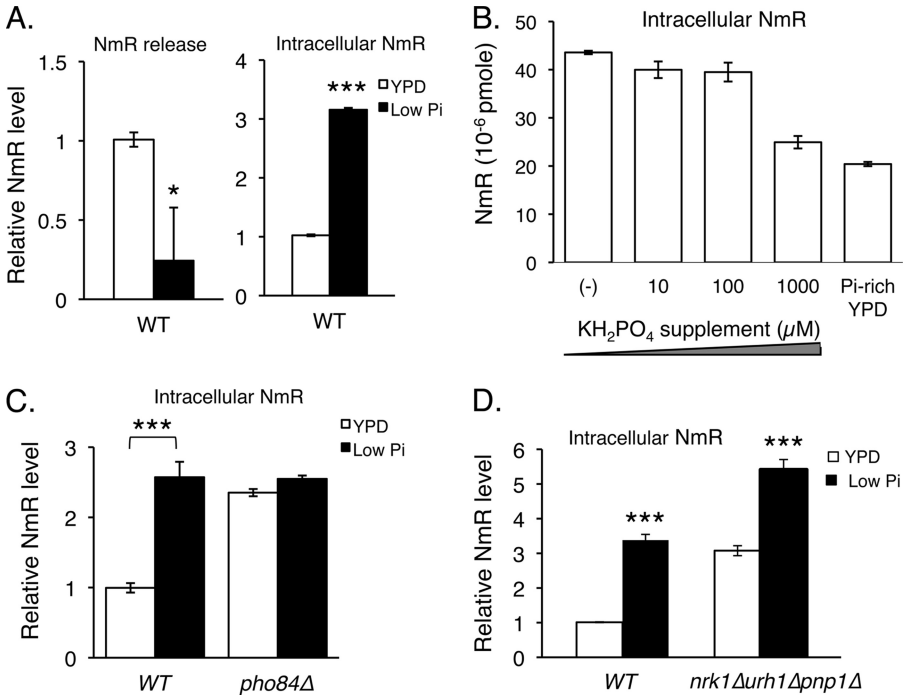

FIGURE 2. **Cellular NmR is modulated by phosphate availability via the *PHO* pathway.** *A*, the cell releases less NmR and retains more NmR in response to P_i limitation. For *A–D*, the levels of NmR are determined by supplementing reporter cells with cell extracts (for intracellular NmR) or culture supernatants (for released NmR) prepared from the strains of interest. *B*, intracellular NmR levels inversely correlate with P_i availability in growth medium. Low-P_i medium is supplemented with various amount of KH_2PO_4 to establish different phosphate availabilities. Regular YPD is used as high-P_i control, which has been reported to contain 2∼5 mM orthophosphate (59, 60). −, no KH_2PO_4 supplement. *C*, the *pho84*Δ mutant grown in YPD shows similar elevated intracellular NmR level as the WT grown in Low-P_i medium. P_i limitation does not further increase the NmR level of the *pho84*Δ mutant. *D*, the *nrk1*Δ*urh1*Δ*pnp1*Δ mutant also responds to low P_i availability and shows increased intracellular NmR. For *A*, *C*, and *D*, relative NmR levels are shown; the growth (A_{600}) of reporter cells is normalized to the set supplemented with cell extracts (or culture supernatant) of WT cells grown in YPD. Results of one representative set of three independent experiments are shown. The *p* values are calculated using Student's *t* test (*, $p < 0.05$; ***, $p < 0.005$).

The PHO-regulated Pho8 Alkaline Phosphatase Is an NmR-producing Enzyme—The positive correlation between NmR levels and *PHO* pathway activities suggested that NmR might be generated by a *PHO*-regulated factor(s), in particular the *PHO*-regulated phosphatase(s). We have previously reported that the periplasmic acid phosphatase Pho5 could mediate the conversion of exogenous NMN to NmR for subsequent uptake and assimilation (11). However, Pho5 appeared to be dispensable for endogenous NmR production because the deletion of Pho5 did not affect intracellular the NmR level (data not shown). The *PHO*-regulated alkaline phosphatase Pho8 functions to scavenge P_i from phosphate-containing molecules intracellularly (40–42). We found that the level of NmR was significantly reduced in the *pho8*Δ mutant (Fig. 3*A*), suggesting Pho8 might play an important role in NmR production. Two 5′ nucleotidases Isn1 and Sdt1 have been reported to generate NmR and NaR from NMN and NaMN, respectively (12). The enzyme Isn1 was first identified as an inosine 5′-monophosphate (IMP)-specific nucleotidase mediating the production of inosine in purine salvage pathway (43). The function of Sdt1 protein was first related to the suppression of 6-azauracil sensitivity of yeast (44) and later characterized as a specific pyrimidine 5′-nucleotidase (45). To gain a better understanding of NmR production, we examined the role of Isn1 and Sdt1 in the determination of intracellular NmR level as a comparison. Under our assay conditions, deletions of Isnl and Sdtl only slightly affected intracellular NmR levels (Fig. 3*A*). This result indicates that out methods may not be sensitive enough to reflect intracellular NmR levels *in vivo*. Our LC-mass spectrometry analysis further confirmed that the level of NmR was substantially reduced in the *pho8*Δ mutant (Fig. 3*B*, *left panel*). Moreover, this reduction of NmR was accompanied by concomitant increases in NMN and NAD$^+$ in the *pho8*Δ mutant (Fig. 3*B*, *right panel*).

We next determined whether Pho8 could mediate NmR production from NMN *in vitro*. Because Pho8 is a vacuolar membrane-located enzyme whose activation requires vacuolar peptidase (46), we employed a cell extract-based alkaline phosphatase activity assay (35) in conjunction with our reporter bioassay ("Experimental Procedures") to determine Pho8-dependent NmR production activity. As shown in Fig. 3*C*, WT cell extract indeed exhibited NMN phosphatase activity that resulted in NmR production in the alkaline phosphatase activity reaction (Fig. 3*C*). Deleting Pho8 completely reduced this NMN-dependent NmR-producing activity, whereas deleting the cytosolic alkaline phosphatase Pho13 had no effect (Fig. 3*C*). This Pho8-dependent NMN phosphatase activity was further confirmed by LC-mass spectrometry analysis of the alkaline phosphatase activity reaction products (Fig. 3*D*). Because the *pho8*Δ mutant also showed decreased NaR and increased NaMN levels (Fig. 3*B*, *right panel*), it is possible that Pho8 could also contribute to the production of NaR from NaMN. As shown in Fig. 3*E*, a Pho8-dependent NaMN phosphatase activity was observed in WT cell extract. These results suggested that Pho8 might function as a NMN and NaMN phosphatase.

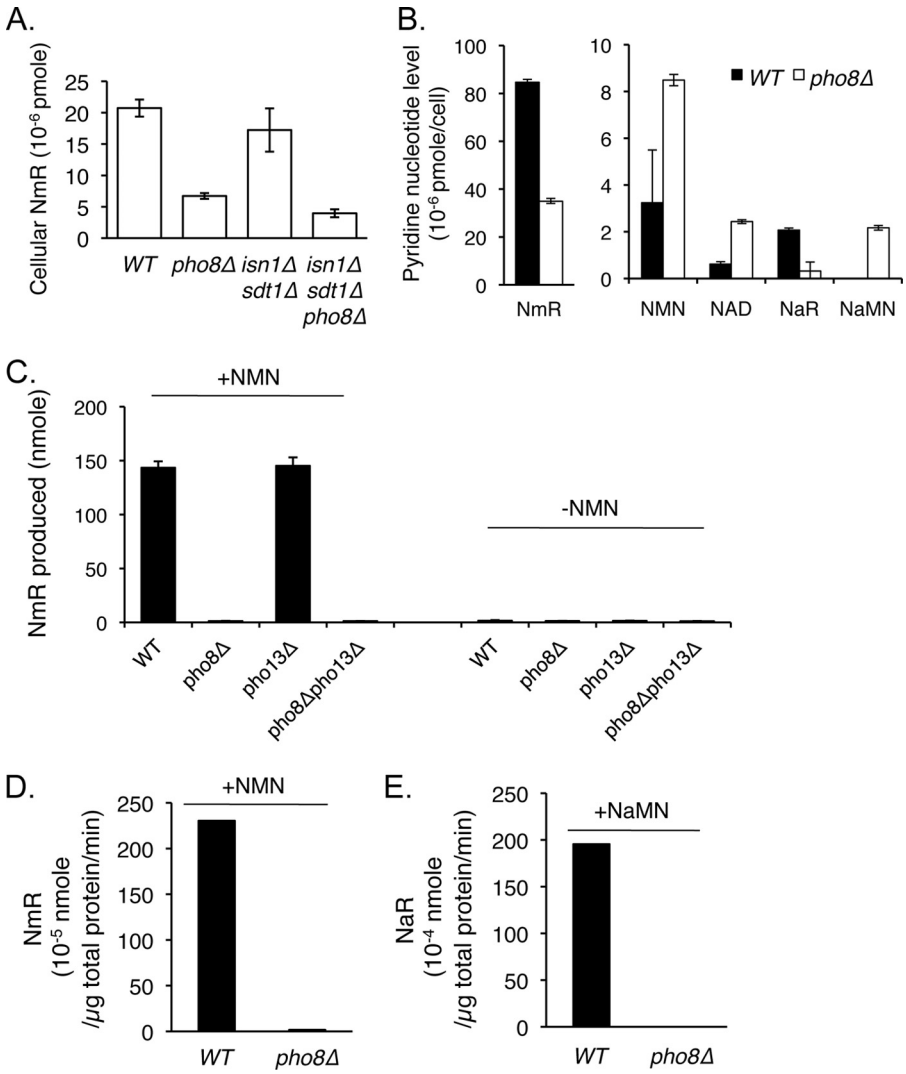

FIGURE 3. **Pho8 plays an important role in NmR production.** *A*, deleting Pho8 (a *PHO*-regulated alkaline phosphatase) significantly reduces intracellular NmR level determined by cross-feeding bioassays. *B*, deleting Pho8 reduces intracellular NmR levels determined by LC-mass spectrometry. *C*, and *D*, yeast cell extracts show Pho8-dependent NMN phosphatase activities to produce NmR determined by cross-feeding bioassays (*C*) and LC-mass spectrometry (*D*). *E*, yeast cell extracts also show Pho8-dependent NaMN phosphatase activities to produce NaR determined by LC-mass spectrometry. Results of one representative set of experiment are shown.

Fun26 Is a Vacuolar NmR Transporter—Because Pho8 is localized to the vacuole, we examined how yeast cells may deliver NmR produced in the vacuole to the cytosol for assimilation. The Fun26 protein was reported to have a minor role in NmR transport relative to Nrt1 (36). However, we found that the *fun26*Δ mutant displayed a comparable level of NmR release to that seen for the *nrt1*Δ mutant (Fig. 4*A*) (Group I, supplemental Table 1). In addition, a significant increase in intracellular NmR level was also observed in the *fun26*Δ mutant but not in the *nrt1*Δ mutant (Fig. 4*B*). Fun26 is the only yeast homolog of the human equilibrative nucleoside transporter (hENT) protein family, which mediates bi-directional transport of specific nucleosides across plasma membrane and intracellular membranes (47–49). Unlike the plasma membrane NmR transporter Nrt1 (36), Fun26 has been suggested to localize to intracellular membranes including vacuolar membranes (50, 51). This may explain why the *fun26*Δ and *nrt1*Δ mutants have distinct phenotypes. To further understand the role of Fun26 in NmR transport, we first determined the cellular localization of Fun26. Adding a GFP tag to Fun26 did not compromise its function, as determined by cross-feeding assays (Fig. 4*C*, *lower panel*). In line with previous reports, Fun26-GFP was clearly localized to the vacuolar membrane (Fig. 4*C*, *upper panels*). Interestingly, deleting the vacuolar resident Pho8 strongly reduced the accumulation of intracellular NmR in the *fun26*Δ mutant (Fig. 4*D*), further supporting the idea that Fun26 is a vacuolar NmR transporter that functions to balance NmR levels between the cytosol and vacuole (Fig. 4*E*).

The Level of NaMN Modulates the PHO Signaling Activity—We have previously shown that assimilation of extracellular NMN requires prior conversion to NmR by the phosphatase Pho5 in the periplasmic space (11). Therefore, in addition to modulating intracellular NmR production, the *PHO* signaling pathway might also modulate extracellular NmR production. Indeed, growth of the NAD$^+$ auxotrophic *qns1*Δ mutant on exogenous NMN was dependent on the *PHO*-regulated transcription factor Pho4 (Fig. 5*A*). In addition, genetically activating *PHO* signaling by deleting Pho84 resulted in significant

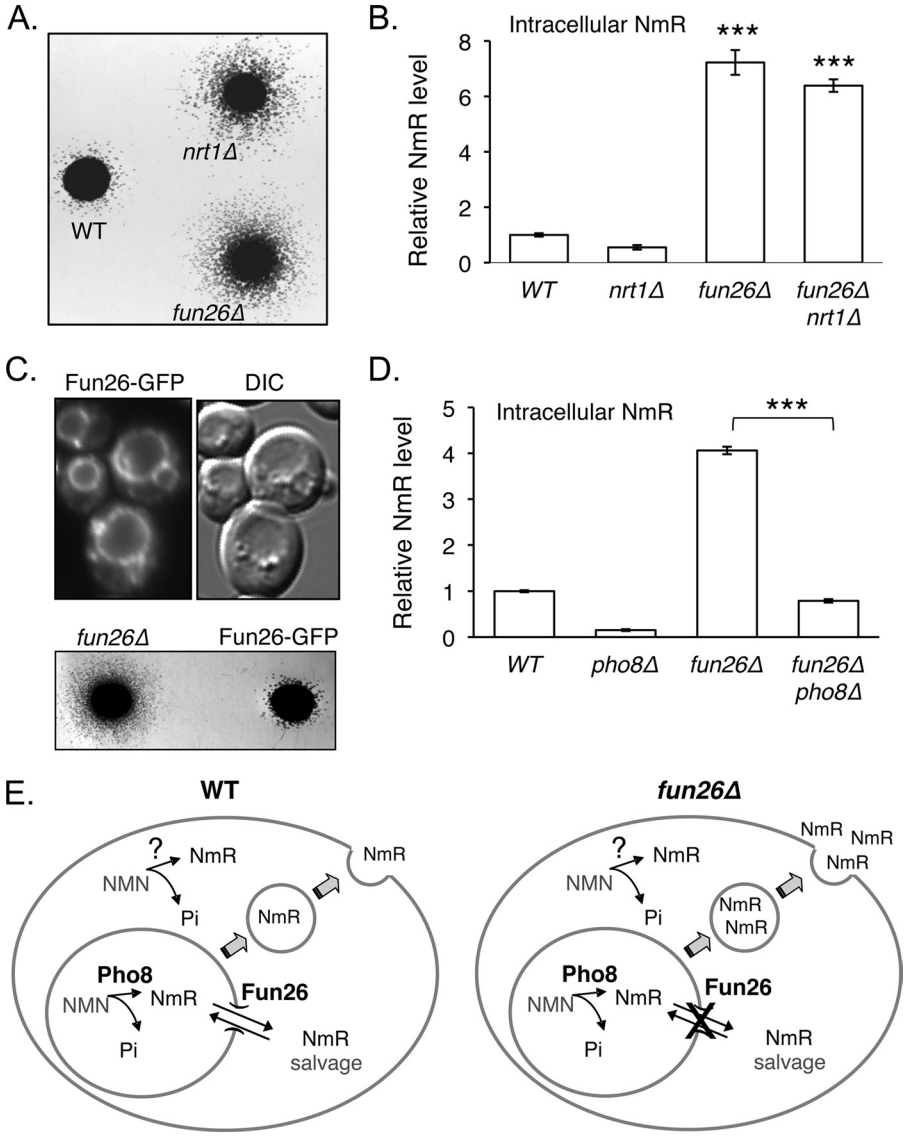

FIGURE 4. **Fun26 is a vacuolar NmR transporter.** *A*, both *fun26*Δ and *nrt1*Δ mutants show increased NmR release determined by the cross-feeding plate assay as described in Fig. 1*C*. *B*, the *fun26*Δ mutant, but not *nrt1*Δ mutant, has high levels of intracellular NmR. *C*, cellular localization of Fun26-GFP protein is shown. The fluorescence signal of Fun26-GFP along with the differential interference contrast (*DIC*) image indicates that Fun26 localizes to vacuolar membrane. Adding a GFP tag to Fun26 does not interfere with its function determined by cross-feeding plate assay (*lower panel*). *D*, deletion of vacuolar resident protein Pho8 significantly lowers intracellular accumulation of NmR in the *fun26*Δ mutant. *E*, the proposed model of the role of Fun26 in NmR metabolism is shown. Fun26 may function to balance NmR between the cytosolic and vacuolar pools (*left*). In Fun26-defective cells, NmR generated in the vacuole cannot be salvaged by NmR assimilation enzymes localized in the cytosol and/or nucleus (*right*). We surmise that accumulated NmR might be delivered to extracellular environment with other cargos in vacuolar-derived vesicles. The accumulation of NmR within the vacuole and vesicles might account for the high level of intracellular NmR detected in the *fun26*Δ mutant. The *p* values are calculated using Student's *t* test (***, $p < 0.005$).

cell growth on NMN 20 h after inoculation when the parental *qns1*Δ mutant still exhibited no cell growth (Fig. 5*B*). These results suggest that the activities of the *PHO* pathway correlate with the time period required for the initiation of growth under this condition. Hence, the initiation time needed for *PHO*-dependent growth could be used to determine the activation status of the *PHO* pathway in strains of interest. However, because the *PHO* signaling cascade is mainly de-repressed by P_i starvation, it is unclear how the *PHO* pathway could be activated in Pi-rich medium, which was used for the growth assay of the *qns1*Δ strains (Fig. 5, *A* and *B*). Because our studies showed that *PHO* signaling and NAD$^+$ metabolism are closely connected, it was possible that the changes of NAD$^+$ and/or specific NAD$^+$ intermediates in the *qns1*Δ mutant triggered *PHO* activation. To test this possibility, we deleted NA/Nam salvage enzymes in the *qns1*Δ mutant to see whether putatively altered levels of specific NAD$^+$ intermediates would affect the *PHO*-dependent growth of the *qns1*Δ mutant. We found that deleting *NPT1* significantly shortened the lag time preceding growth initiation of the *qns1*Δ mutant from ~24 to ~14 h (Fig. 5*C*).

Next, we examined whether deleting these NA/Nam salvage enzymes in wild-type background would be sufficient to activate the *PHO* pathway. As shown in Fig. 5, *D* and *E*, the *npt1*Δ mutant exhibited higher Pho5 activity as determined by both colorimetric acid phosphatase plate assay and liquid assay (32). Deleting *TNA1* or *PNC1* also slightly increased Pho5 activity. Although Npt1, Tna1, and Pnc1 contribute to the production of NaMN and NAD$^+$ (Fig. 6*A*), observed *PHO* activation in these

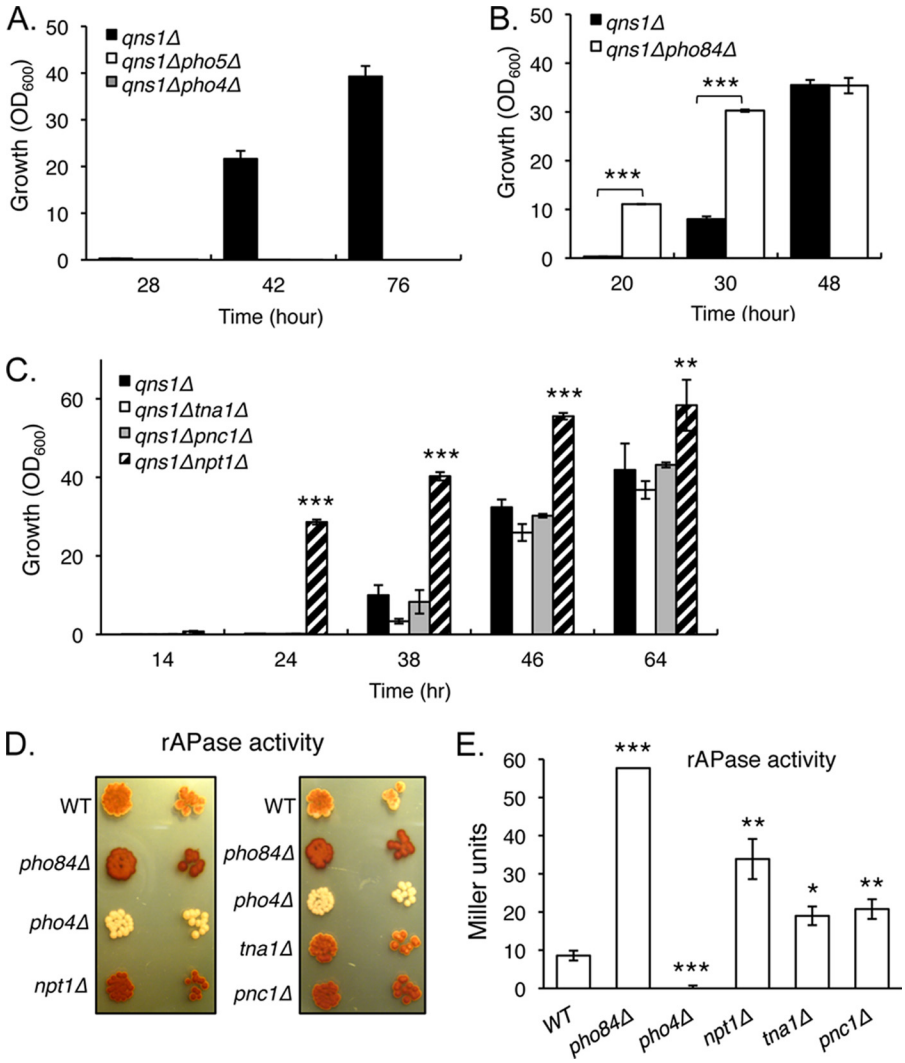

FIGURE 5. **Genetic analysis of the role of NAD$^+$ metabolism in the activation of the *PHO* pathway.** *A*, *PHO*-dependent NMN assimilation in the *qns1*Δ mutant. For *A*, *B*, and *C*, all strains are inoculated into YPD medium containing 50 μM NMN at a starting A_{600} of 0.05. "*Growth* (OD_{600})" on the *y* axis refers to the growth of the indicated strains over time. Because all these strains harbor a *qns1*Δ deletion (lacking NAD$^+$ synthetase), these cells would not grow unless NmR or NMN is present in the growth medium. Growth on exogenous NMN relies on *PHO*-activated phosphatase Pho5 to acquire absorbable NmR (11); therefore, the extent of cell growth under this condition reflects the level of *PHO* activity. *B*, deleting Pho84 in the *qns1*Δ mutant results in significant growth at 20 h after inoculation when the *qns1*Δ mutant still exhibits no cell growth. *C*, deleting Npt1 significantly shortens the lag time preceding growth initiation of the *qns1*Δ mutant from ~24 to ~14 h. For *D* and *E*, the repressible acid phosphatase (*rAPase*) activity is significantly increased in the *npt1*Δ mutant and modestly elevated in the *tna1*Δ and *pnc1*Δ mutants as determined by colorimetric plate assay (*D*) and liquid assay (*E*). For *E*, cells grown to late log phase are harvested for repressible acid phosphatase activity assay. Repressible acid phosphatase activities are expressed in Miller units ((A_{420} × 1000)/(A_{600} × volume of cells harvested) × 15 min). The *p* values are calculated using Student's *t* test (*, $p < 0.05$; **, $p < 0.01$; ***, $p < 0.005$).

mutants (Fig. 5, *C*, *D*, and *E*) was unlikely due to NAD$^+$ depletion because Pnc1 deletion does not decrease NAD$^+$ level (11, 52). Therefore, we tested whether enhanced *PHO* activation might be due to NaMN depletion by LC-mass spectrometry analysis. Fig. 6*B* showed that the level of NaMN was decreased by deleting Npt1 in the *qns1*Δ mutant. In addition, the level of NmR was concomitantly increased (Fig. 6*B*). This result was expected as deleting Npt1 enhances *PHO* activation (Fig. 5, *C*, *D*, and *E*), which would result in increased NmR production. Further supporting our hypothesis, overexpressing a NaMN producing enzyme Qpt1 alone or in combination with the supplementation of its substrate QA was sufficient to delay the growth of the *qns1*Δ*npt1*Δ mutant (Fig. 6*C*). Collectively, these results demonstrate that NaMN accumulation delays *PHO* activation (Fig. 6, *B* and *C*) and that NaMN depletion enhances *PHO* activation (Fig. 5, *C*, *D*, and *E*). Our studies also suggest that the level of intracellular NaMN might function as a molecular link connecting the *PHO* signaling and NAD$^+$ metabolic pathways. Given that the deletion of *NPT1* leads to increased NmR production in the *qns1*Δ background (Fig. 6*B*), the switch from NA/Nam salvage to NmR salvage in response to changes of growth conditions is also likely to be signaled by intracellular NaMN level.

DISCUSSION

In this study we characterized the *PHO* pathway as a novel component in NAD$^+$/NmR metabolism. Mutants with activated *PHO* signaling showed increased NmR levels, whereas mutants with decreased *PHO* signaling displayed reduced NmR levels. We have also identified alkaline phosphatase Pho8 as a

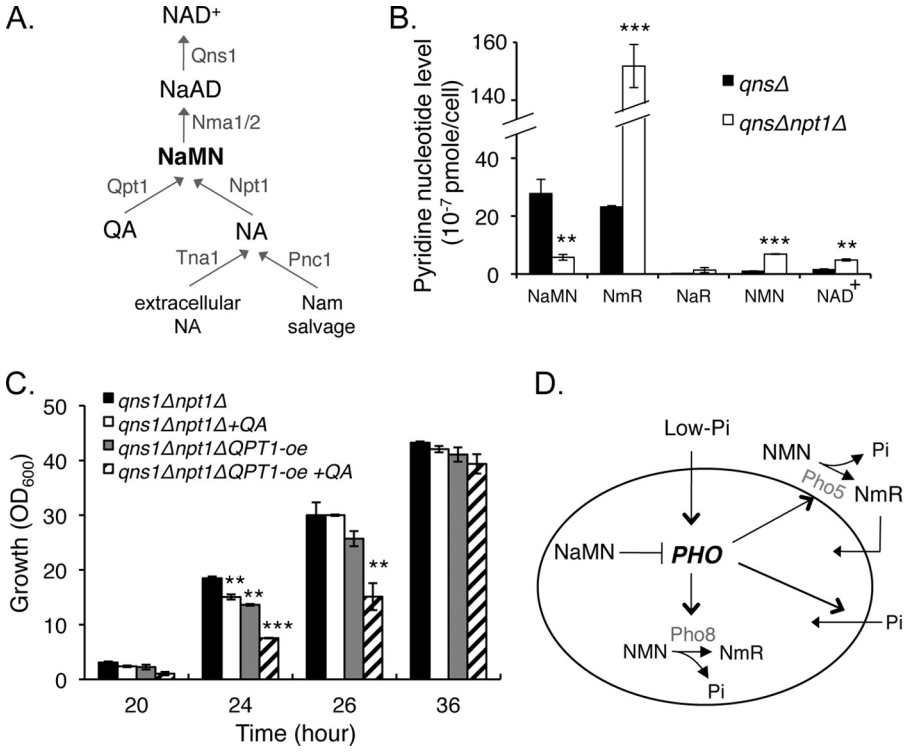

FIGURE 6. **NaMN metabolism modulates the activation of the *PHO* pathway.** *A*, factors that function in the generation of NaMN and in the synthesis of NAD$^+$ from NaMN are shown. *B*, pyridine metabolite analysis of the *qns1*Δ and *qns1*Δ*npt1*Δ mutants is shown. Deleting Npt1 decreases NaMN levels in the *qns1*Δ mutant. Pyridine metabolite levels are determined by LC-mass spectrometry. *C*, overexpressing Qpt1 in combination with QA supplementation delays the *PHO*-dependent growth of the *qns1*Δ*npt1*Δ mutant. QA is supplemented at a concentration of 100 μM. *D*, shown is a proposed model of the interconnection between the *PHO* pathway and NAD$^+$ metabolism. The *PHO* pathway receives signals of P_i availability and cellular NaMN level, which leads to *PHO* responses including P_i acquisition and NMN catabolism. The conversion of NMN to NmR could be mediated by Pho8 in the vacuole and by Pho5 in the periplasmic space of yeast cells. The *p* values are calculated using Student's *t* test (**, $p < 0.01$; ***, $p < 0.005$).

potential important enzyme of NmR production, likely to work by removing P_i from NMN. We demonstrated that the increase in intracellular NmR level is an integral part of the *PHO* response upon P_i limitation, during which cells retain more NmR instead of releasing it extracellularly. By genetically manipulating the enzymes of NA/Nam salvage, we showed that accumulations of NaMN might inhibit *PHO* activation, which also suggested that NaMN might function as an internal signal for the *PHO* pathway (Fig. 6*D*).

The repression and activation of the *PHO* pathway is an important mechanism of cellular adaptation to endure the variation of P_i availability and to maintain metabolic homeostasis. The signals of external P_i level and internal reservoir (including orthophosphate and polyphosphate) are sensed and conveyed by the *PHO* pathway that leads to responses at the gene expression level to adjust cellular activities in P_i transport and scavenging. Although P_i availability appears to be the major signal, recent studies have revealed novel components in the regulatory circuit of the *PHO* responses. It has been shown that, after prolonged P_i starvation, the repletion of P_i to cells leads to degradation of the high affinity phosphate transporter Pho84 (53, 54). This response requires the activation of the protein kinase A (53, 54), demonstrating a connection between the glucose and phosphate signaling pathways. The level of other nutrient intermediates also influences the activation of the *PHO* pathway. Recently, it was reported that the synthesis of purine nucleotide is co-regulated with the *PHO* pathway by a mutual transcription factor Pho2 (24, 25). The accumulation of the purine biosynthetic intermediate, in particular 5′-phosphoribosyl-5-amino-4-imidazole carboxamide (AICAR), activates the transcription of purine regulon genes and *PHO* regulon genes by Pho2 in a P_i availability-independent manner (24, 25). Moreover, deficiency in Adk1 (adenylate kinase 1), an important enzyme in energy metabolism, results in a transcriptional profile similar to the cellular response upon P_i starvation (24, 25).

Our present and earlier studies suggest that NAD$^+$ metabolism is also connected to the *PHO* pathway (Fig. 6*D*). The coupling of these two pathways may render a more efficient metabolic support under specific conditions. For instance, the phosphate moiety of NMN is a putative target for phosphate scavenging during P_i limitation. Indeed, activation of the *PHO* pathway by deleting Pho84 or by decreasing P_i availability in growth medium increases intracellular NmR levels (Figs. 1*E* and 2*B*). Moreover, the increase of intracellular NmR in response to P_i starvation is likely mediated by *PHO*-regulated Pho8, which catalyzes the generation of NmR and releases phosphate from NMN (Fig. 3, *C* and *D*). Similarly, the conversion of NMN to NmR mediated by *PHO*-regulated Pho5 in the periplasmic space also allows cells to acquire both P_i and NmR from an extracellular source (11).

Our results show that the *PHO* pathway also responds to NaMN depletion. The mutant with a deletion of the major NaMN generation enzyme Npt1 showed de-repression of the *PHO* pathway as determined by the acid phosphatase activity assay (Fig. 5, *D* and *E*). The deletion of *NPT*1 stimulates the

PHO pathway-dependent growth of the *qns1*Δ mutant (Fig. 5*C*), whereas overexpression of Qpt1 (which putatively leads to increases of NaMN) inhibits the growth of the *qns1*Δ mutant (Fig. 6*C*). Since NaMN is an important intermediate for NAD$^+$ biosynthesis (Fig. 1*A*), low levels of NaMN might reflect impaired NAD$^+$ biosynthesis and lead to de-repression of an alternative NAD$^+$ salvage route-NmR utilization (Fig. 1*A*). Because NmR-mediated NAD$^+$ synthesis requires phosphate (in form of ATP), a coordinated activation of the *PHO* pathway is important in supporting NAD$^+$ synthesis and homeostasis.

In addition to the *PHO* pathway, our genetic screen also revealed potential novel players in NmR/NAD$^+$ metabolism. We found 12 mutants harboring defects in the regulation or the assembly of vacuolar ATP synthase complex showed strong or moderately higher NmR release (Group I and II, supplemental Table 1). The vacuolar ATP synthase complex is essential in establishing and maintaining the acidity of vacuolar matrix, and the impairment in vacuolar ATP synthase complex will alter the activity of vacuolar proteins, including peptidases and phosphatases (55). The identification of vacuolar ATP synthase assembly mutants in our genetic screen suggests that vacuole is a putative compartment important for NmR homeostasis in yeast. In addition, 19 mutants with deficiencies in the protein trafficking process or in the vesicle-mediated transport machinery were found to release more NmR (Group I and II, supplemental Table 1). One important function of vesicle-mediated transport is to deliver secreted proteins and membrane proteins to their final destinations (56, 57). It is, therefore, possible that the aberrant NmR release might result from defects in the transport of NmR-metabolizing proteins to certain locations; for example, NmR transporter Nrt1 to plasma membrane. A comprehensive characterization of the turnover of Nrt1 would help address the phenotypes of this group of mutants. The identification of phosphatase Pho8 as a NmR-producing enzyme raises another question; if vacuole is a cellular compartment for NmR production, how does cell salvage vacuolar NmR to synthesize NAD$^+$ in other compartments, for example cytosol? Previous reports (50, 51) and our current studies collectively suggest that Fun26 could balance NmR between the cytosolic and vacuolar pools, which would enable the utilization of NmR originated from the vacuole. In addition, the mechanism of NmR export has not yet been addressed. Because the *fun26*Δ mutant also releases more NmR (Fig. 4*A*), it is possible that the increase of NmR release in this mutant is due to the accumulation of NmR in the vacuole. A direct investigation to determine whether NmR molecules could be exported extracellularly, for example, along with other protein cargos through vesicle-mediated transport, would help depict the dynamics of endogenous NmR.

We have previously shown that the ability to salvage both the intracellular and extracellular NmR is important for cell survival and stress resistance (11). To date, the mechanisms of NmR uptake and its transport between cellular compartments in higher eukaryotes are still unknown. Four Fun26-related human ENT proteins have been characterized (47). Given the role of Fun26 in NmR metabolism in yeast, it would be informative to determine whether the plasma membrane-localized hENT1 and hENT2 and lysosome membrane-resided hENT3 also participate in NmR homeostasis and NAD$^+$ metabolism in human.

Acknowledgments—We thank Dr. J. Roth for critical reading of this manuscript, members of the Lin laboratory for discussions and suggestions, and Dr. T. Powers for providing the pFA6a-kanMX6-PGAL1-GFP plasmid. We also thank Dr. J. Engebrecht and Dr. J. Roth for suggestions.

REFERENCES

1. Lin, S. J., Defossez, P. A., and Guarente, L. (2000) *Science* **289,** 2126–2128
2. Lin, S. J., and Guarente, L. (2003) *Curr. Opin. Cell Biol.* **15,** 241–246
3. Rusche, L. N., Kirchmaier, A. L., and Rine, J. (2003) *Annu. Rev. Biochem.* **72,** 481–516
4. Bürkle, A. (2005) *FEBS J.* **272,** 4576–4589
5. Chini, E. N. (2009) *Curr. Pharm. Des.* **15,** 57–63
6. Panozzo, C., Nawara, M., Suski, C., Kucharczyka, R., Skoneczny, M., Bécam, A. M., Rytka, J., and Herbert, C. J. (2002) *FEBS Lett.* **517,** 97–102
7. Preiss, J., and Handler, P. (1958) *J. Biol. Chem.* **233,** 493–500
8. Preiss, J., and Handler, P. (1958) *J. Biol. Chem.* **233,** 488–492
9. Bieganowski, P., and Brenner, C. (2004) *Cell* **117,** 495–502
10. Belenky, P., Racette, F. G., Bogan, K. L., McClure, J. M., Smith, J. S., and Brenner, C. (2007) *Cell* **129,** 473–484
11. Lu, S. P., Kato, M., and Lin, S. J. (2009) *J. Biol. Chem.* **284,** 17110–17119
12. Bogan, K. L., Evans, C., Belenky, P., Song, P., Burant, C. F., Kennedy, R., and Brenner, C. (2009) *J. Biol. Chem.* **284,** 34861–34869
13. Sporty, J., Lin, S. J., Kato, M., Ognibene, T., Stewart, B., Turteltaub, K., and Bench, G. (2009) *Yeast* **26,** 363–369
14. Lenburg, M. E., and O'Shea, E. K. (1996) *Trends Biochem. Sci.* **21,** 383–387
15. Oshima, Y. (1997) *Genes Genet. Syst.* **72,** 323–334
16. Persson, B. L., Lagerstedt, J. O., Pratt, J. R., Pattison-Granberg, J., Lundh, K., Shokrollahzadeh, S., and Lundh, F. (2003) *Curr. Genet.* **43,** 225–244
17. Auesukaree, C., Tochio, H., Shirakawa, M., Kaneko, Y., and Harashima, S. (2005) *J. Biol. Chem.* **280,** 25127–25133
18. Lee, Y. S., Mulugu, S., York, J. D., and O'Shea, E. K. (2007) *Science* **316,** 109–112
19. Lee, Y. S., Huang, K., Quiocho, F. A., and O'Shea, E. K. (2008) *Nat. Chem. Biol.* **4,** 25–32
20. Ueda, Y., and Oshima, Y. (1975) *Mol. Gen. Genet.* **136,** 255–259
21. Bun-Ya, M., Nishimura, M., Harashima, S., and Oshima, Y. (1991) *Mol. Cell. Biol.* **11,** 3229–3238
22. Wykoff, D. D., and O'Shea, E. K. (2001) *Genetics* **159,** 1491–1499
23. Auesukaree, C., Homma, T., Tochio, H., Shirakawa, M., Kaneko, Y., and Harashima, S. (2004) *J. Biol. Chem.* **279,** 17289–17294
24. Gauthier, S., Coulpier, F., Jourdren, L., Merle, M., Beck, S., Konrad, M., Daignan-Fornier, B., and Pinson, B. (2008) *Mol. Microbiol.* **68,** 1583–1594
25. Pinson, B., Vaur, S., Sagot, I., Coulpier, F., Lemoine, S., and Daignan-Fornier, B. (2009) *Genes Dev.* **23,** 1399–1407
26. Brachmann, C. B., Davies, A., Cost, G. J., Caputo, E., Li, J., Hieter, P., and Boeke, J. D. (1998) *Yeast* **14,** 115–132
27. Easlon, E., Tsang, F., Skinner, C., Wang, C., and Lin, S. J. (2008) *Genes Dev.* **22,** 931–944
28. Rubin, G. M. (1973) *J. Biol. Chem.* **248,** 3860–3875
29. Winzeler, E. A., Shoemaker, D. D., Astromoff, A., Liang, H., Anderson, K., Andre, B., Bangham, R., Benito, R., Boeke, J. D., Bussey, H., Chu, A. M., Connelly, C., Davis, K., Dietrich, F., Dow, S. W., El Bakkoury, M., Foury, F., Friend, S. H., Gentalen, E., Giaever, G., Hegemann, J. H., Jones, T., Laub, M., Liao, H., Liebundguth, N., Lockhart, D. J., Lucau-Danila, A., Lussier, M., M'Rabet, N., Menard, P., Mittmann, M., Pai, C., Rebischung, C., Revuelta, J. L., Riles, L., Roberts, C. J., Ross-MacDonald, P., Scherens, B., Snyder, M., Sookhai-Mahadeo, S., Storms, R. K., Véronneau, S., Voet, M., Volckaert, G., Ward, T. R., Wysocki, R., Yen, G. S., Yu, K., Zimmermann, K., Philippsen, P., Johnston, M., and Davis, R. W. (1999) *Science* **285,** 901–906
30. Sporty, J. L., Kabir, M. M., Turteltaub, K. W., Ognibene, T., Lin, S. J., and Bench, G. (2008) *J. Sep. Sci.* **31,** 3202–3211

31. Evans, C., Bogan, K. L., Song, P., Burant, C. F., Kennedy, R. T., and Brenner, C. (2010) *BMC Chem. Biol.* **10,** 2
32. To-E, A., Ueda, Y., Kakimoto, S. I., and Oshima, Y. (1973) *J. Bacteriol.* **113,** 727–738
33. Neef, D. W., and Kladde, M. P. (2003) *Mol. Cell. Biol.* **23,** 3788–3797
34. Longtine, M. S., McKenzie, A., 3rd, Demarini, D. J., Shah, N. G., Wach, A., Brachat, A., Philippsen, P., and Pringle, J. R. (1998) *Yeast* **14,** 953–961
35. Noda, T., and Klionsky, D. J. (2008) *Methods Enzymol.* **451,** 33–42
36. Belenky, P. A., Moga, T. G., and Brenner, C. (2008) *J. Biol. Chem.* **283,** 8075–8079
37. Grubmeyer, C. T., Gross, J. W., and Rajavel, M. (1999) *Methods Enzymol.* **308,** 28–48
38. Emanuelli, M., Carnevali, F., Lorenzi, M., Raffaelli, N., Amici, A., Ruggieri, S., and Magni, G. (1999) *FEBS Lett.* **455,** 13–17
39. Brachmann, C. B., Sherman, J. M., Devine, S. E., Cameron, E. E., Pillus, L., and Boeke, J. D. (1995) *Genes Dev.* **9,** 2888–2902
40. Toh-E, A., Nakamura, H., and Oshima, Y. (1976) *Biochim. Biophys. Acta* **428,** 182–192
41. Kaneko, Y., Hayashi, N., Toh-e, A., Banno, I., and Oshima, Y. (1987) *Gene* **58,** 137–148
42. Clark, D. W., Tkacz, J. S., and Lampen, J. O. (1982) *J. Bacteriol.* **152,** 865–873
43. Itoh, R., Saint-Marc, C., Chaignepain, S., Katahira, R., Schmitter, J. M., and Daignan-Fornier, B. (2003) *BMC Biochem.* **4,** 4
44. Shimoaraiso, M., Nakanishi, T., Kubo, T., and Natori, S. (2000) *J. Biol. Chem.* **275,** 29623–29627
45. Nakanishi, T., and Sekimizu, K. (2002) *J. Biol. Chem.* **277,** 22103–22106
46. Klionsky, D. J., and Emr, S. D. (1989) *EMBO J.* **8,** 2241–2250
47. Young, J. D., Yao, S. Y., Sun, L., Cass, C. E., and Baldwin, S. A. (2008) *Xenobiotica* **38,** 995–1021
48. Baldwin, S. A., Yao, S. Y., Hyde, R. J., Ng, A. M., Foppolo, S., Barnes, K., Ritzel, M. W., Cass, C. E., and Young, J. D. (2005) *J. Biol. Chem.* **280,** 15880–15887
49. Endo, Y., Obata, T., Murata, D., Ito, M., Sakamoto, K., Fukushima, M., Yamasaki, Y., Yamada, Y., Natsume, N., and Sasaki, T. (2007) *Cancer Sci.* **98,** 1633–1637
50. Vickers, M. F., Yao, S. Y., Baldwin, S. A., Young, J. D., and Cass, C. E. (2000) *J. Biol. Chem.* **275,** 25931–25938
51. Wiederhold, E., Gandhi, T., Permentier, H. P., Breitling, R., Poolman, B., and Slotboom, D. J. (2009) *Mol. Cell. Proteomics* **8,** 380–392
52. Sandmeier, J. J., Celic, I., Boeke, J. D., and Smith, J. S. (2002) *Genetics* **160,** 877–889
53. Mouillon, J. M., and Persson, B. L. (2005) *Curr. Genet.* **48,** 226–234
54. Lundh, F., Mouillon, J. M., Samyn, D., Stadler, K., Popova, Y., Lagerstedt, J. O., Thevelein, J. M., and Persson, B. L. (2009) *Biochemistry* **48,** 4497–4505
55. Li, S. C., and Kane, P. M. (2009) *Biochim. Biophys. Acta* **1793,** 650–663
56. Bonifacino, J. S., and Glick, B. S. (2004) *Cell* **116,** 153–166
57. Robinson, M. S. (2004) *Trends Cell Biol.* **14,** 167–174
58. Revollo, J. R., Grimm, A. A., and Imai, S. (2007) *Curr. Opin. Gastroenterol.* **23,** 164–170
59. Bisson, L. F., and Thorner, J. (1982) *Genetics* **102,** 341–359
60. Werner, T. P., Amrhein, N., and Freimoser, F. M. (2005) *Arch. Microbiol.* **184,** 129–136